# ETS variant transcription factor 6 enhances oxidized low-density lipoprotein-induced inflammatory response in atherosclerotic macrophages via activating NF-κB signaling

## Xiaofang Xiong[1] ⬤, Zheng Yan[1], Wei Jiang[1] and Xuejun Jiang[2]

## Abstract

**Objectives**: Macrophages play a critical role in atherosclerosis by contributing to plaque development, local inflammation, and thrombosis. Elucidation of the molecular cascades in atherosclerotic macrophages is important for preventing and treating atherosclerosis. This study aims to deepen the understanding of the mechanisms that regulate the function of aorta macrophage in atherosclerosis. **Methods**: In the current study, the expression and function of ETS variant transcription factor 6 (ETV6) in aorta macrophages in a mouse atherosclerosis model. Aorta macrophages were enriched by flow cytometry. ETV6 expression was analyzed by quantitative RT-PCR. The role of ETV6 in macrophage-mediated pro-inflammatory response was evaluated both *in vitro* and *in vivo* after ETV6 silencing. **Results:** A remarkable elevation of ETV6 in aorta macrophages of atherosclerotic mice was observed. In addition, *in vitro* analysis indicated that oxidized low-density lipoprotein (oxLDL) up-regulated ETV6 in macrophages via the NF-κB pathway. ETV6 silencing suppressed oxLDL-induced expression of IL-1β, IL-6, and TNF-α in macrophages *in vitro*. However, ETV6 silencing did not impact the uptake of either oxLDL or cholesterol by macrophages. Furthermore, ETV6 silencing suppressed oxLDL-induced activation of the NF-κB pathway in macrophages, as evidenced by less phosphorylation of IKKβ and NF-κB p65, more cytoplasmic IκBα, and lower nuclear NF-κB p65. Moreover, ETV6 silencing inhibited the production of IL-1β and TNF-α in aorta macrophages *in vivo*. **Conclusion:** ETV6 supports macrophage-mediated inflammation in atherosclerotic aortas. This is a novel mechanism regulating the pro-inflammatory activity of atherosclerotic macrophages.

## Keywords

atherosclerosis, macrophages, ETS variant transcription factor 6, oxidized low-density lipoprotein, inflammation

## Introduction

Atherosclerosis is characterized by unbalanced lipid metabolism and pathological immune responses mediated by macrophages and other immune cell populations.[1,2] Low-density lipoprotein (LDL), especially its modified form, is a primary source of lipid accumulation in atherosclerotic lesions. During the formation of atherosclerotic lesions, blood-derived monocytes transmigrate into and settle into atherosclerotic lesions, where they differentiate into macrophages and engulf lipoproteins through macropinocytosis or scavenger receptor-mediated uptake.

[1]The Department of Cardiology, Wuhan Third Hospital (Tongren Hospital of Wuhan University), Wuchang, Hubei, China
[2]The Department of Cardiology, Renmin Hospital of Wuhan University (Hubei Gneral Hospital), Wuchang, Hubei, China

**Corresponding authors:**
Xiaofang Xiong, The Department of Cardiology, Wuhan Third Hospital (Tongren Hospital of Wuhan University), 241 Pengliuyang Road, Wuchang, Hubei 430060, China.
Email: xxf104622930@outlook.com

Xuejun Jiang, The Department of Cardiology at Renmin Hospital of Wuhan University (Hubei Gneral Hospital), 238 Jiefang Road, Wuchang, Hubei 430060, China.
Email: xjjiang@whu.edu.cn

LDL is considered the major source of excess cholesterol deposits in macrophages. Exorbitant aggregation of cholesterol in the cytosol of macrophages initiates the development of cholesterol crystals and consequently activates the inflammatory pathways especially the NLRP3 inflammasome signaling and endoplasmic reticulum stress.[3,4] To prevent and treat atherosclerosis, it is essential to elucidate the molecular cascades and factors that modulate the function of macrophages in atherosclerotic plaques.

Our unpublished preliminary transcriptomic analysis reveals an increase in ETS variant transcription factor 6 (ETV6) in aorta macrophages in atherosclerotic mice (data not shown). Therefore, we wanted to further evaluate ETV6 expression and its role in the macrophage-mediated pathological progression of atherosclerosis. In the human genome, the *ETV6* gene resides on chromosome 12 and encodes a transcription factor of the ETS family.[5] The ETV6 protein possesses three domains essential for hematopoiesis.[5] ETV6 gene mutations cause susceptibility to myelodysplastic syndromes and acute leukemia.[6,7] Germline ETV6 variations could be a susceptibility factor for hematologic malignancies. However, to our knowledge, the significance of ETV6 to the development and function of macrophages has not been understood.

In this mouse atherosclerosis study, we evaluated the expression of ETV6 in atherosclerotic macrophages and its effect on the inflammatory reaction of macrophages. Our data unveiled the role of ETV6 in supporting macrophage-mediated inflammation in atherosclerotic aortas.

## Materials and methods

### Atherosclerosis model

The animal experiments were approved by the Wuhan University Animal Care and Use Committee. All procedures were carried out in compliance with the Wuhan University Guidelines for the Use of Animals. Eight-week-old male C57BL/6J and apolipoprotein E-deficient (ApoE$^{-/-}$) mice were obtained from Beijing Biocytogen Co., Ltd. The ApoE$^{-/-}$ mice were given a high-fat diet containing 0.2% cholesterol and 21% fat by weight for 16 weeks until atherosclerotic lesions were developed in the aortas.

### Oil red O staining

Aortas were fixed in 4% formaldehyde, rinsed with water, and stained with 5% oil red O (Sigma-Aldrich) for 30 min. The aortas were then washed three times (15 s each) in running distilled water. Finally, the aortas were photographed using a digital camera to acquire images.

### Isolation of aorta cells and splenocytes

Aorta cells were obtained based on previously published protocols.[8,9] After anesthesia using 2% halothane, mice were perfused with 2 mL of saline through cardiac puncture. The aorta and its branches were taken, cut into pieces, and digested in 100 μL of RPMI1640 supplemented with 10% fetal bovine serum (FBS), 400 U/ml collagenase I, 150 U/ml collagenase XI, 50 U/ml hyaluronidase I-s, and 50 U/ml DNase I at 37°C for 30 min on an orbital shaker. The digested tissue was gently pipetted five times and then filtered through a cell strainer to prepare a single-cell suspension. After centrifugation at 250×g for 5 min, the cell pellet was resuspended in 200 μL of ice-cold PBS before further processing. In some experiments, aortas from 9 to 10 mice were pooled for digestion and the reagents were scaled up proportionally.

Splenocytes were prepared by grinding a spleen in a 70-μm cell strainer containing 1 mL of phosphate-buffered saline (PBS). Red blood cells were removed by incubation in Tris-buffered ammonium chloride. Cells were washed with PBS once and subjected to analysis.

### Fluorescence-activated cell sorting (FACS)

The following fluorochrome-labeled anti-mouse antibodies were purchased from Biolegend: PE/Cy7 anti-CD3 (17A2), PE/Cy7 anti-NK1.1 (PK136), PE/Cy7 anti-CD19 (6D5), PE/Cy7 anti-CD11c (N418), APC anti-CD11b (M1/70), PE/Cy7 anti-Gr1 (RB6-8C5), PE anti-F4/80 (T45-2342), APC/Cy7 anti-Ly-6C (AL-21), and APC anti-CD45 (30-F11). Cells were incubated in PBS containing 5 μg/ml of each antibody for 30 min on ice. Cells were then washed with PBS twice, analyzed on a BD LSRII flow cytometer, or sorted on a BD FACSAria cell sorter (Both from BD Biosciences). Cell

**Table 1.** Primer sequences.

| Target | Sense (5′ to 3′) | Anti-sense (5′ to 3′) |
|---|---|---|
| ETV6 | TGCCTTTCAAAACCACCCCT | TAGCCTCTATGTGCCCCACT |
| TNF-α | GCCTCTTCTCATTCCTGCTTG | CTGATGAGAGGGAGGCCATT |
| IL-1β | TGTCTGACCCATGTGAGCTG | GCCACAGGGATTTTGTCGTT |
| IL-6 | ACTTCACAAGTCGGAGGCTT | TTCTGACAGTGCATCATCGCT |
| IL-10 | AGGCGCTGTCATCGATTTCT | ATGGCCTTGTAGACACCTTGG |
| TGF-β1 | CTGCTGACCCCCACTGATAC | GTGAGCGCTGAATCGAAAGC |
| β-actin | ACAACCTTCTTGCAGCTCCTC | CTGACCCATACCCACCATCAC |

apoptosis was determined using the Annexin V APC Apoptosis Detection Kit (eBioscience) following the vendor's manual.

## Reverse transcription and quantitative polymerase chain reaction (RT-qPCR)

RNAs were enriched using the RNAprep pure Micro Kit (Tiangen Biotech) following the supplier's manual. cDNAs were synthesized using the BeyoRT™ III First Strand cDNA Synthesis Kit (Beyotime Biotech). The Talent qPCR PreMix (Tiangen Biotech) was used for the quantitative PCR on a LightCycler® 480 System (Roche). The primers are shown in Table 1. The fold changes of relevant mRNAs were calculated by the $2^{-\Delta\Delta Ct}$ method.

## Immunofluorescence staining

Aortas were fixed in 4% formaldehyde for 24 h, dehydrated overnight, and embedded in paraffin. Paraffin cross-sections (4-μm thick) were prepared. After incubation with 5% normal goat serum for 1 h at room temperature, the sections were incubated with rabbit anti-ETV6 antibody (1:200, PA5-109,697, Thermo Fisher Scientific) and rat anti-F4/80 (10 μg/ml, ab6640, Abcam) overnight at 4ºC. After three washes with PBS, the samples were incubated with 5 μg/ml Alexa Fluor® 488-conjugated goat anti-rat IgG H&L and Alexa Fluor® 594-conjugated goat anti-rabbit IgG H&L (1:1000, ab150157, ab150080, Abcam) for an hour at room temperature. For Immunofluorescence cytochemistry, macrophages were fixed in acetone for 10 min and incubation with 5% normal goat serum for 1 h at room temperature. Macrophages were then incubated with NF-κB p65 antibody (1:500, #8242, Cell Signaling Technology) overnight at 4ºC. After three washes with PBS, cells were incubated with Alexa Fluor® 488-conjugated goat anti-rabbit IgG H&L (1:1000, ab150077, Abcam) for an hour at room temperature. Cells were washed and incubated in the mounting medium with DAPI (ab104139, Abcam). The samples were observed and photographed on a Leica DM500 fluorescence microscope (Leica).

## Aorta macrophage culture and in vitro treatment

$1\times10^6$/ml aorta macrophages were exposed to 50 μg/mL oxLDL (Yeasen Biotech) or 100 ng/mL lipopolysaccharide (LPS, Sigma-Aldrich) in the presence or absence of 5 μM NF-κB inhibitor QNZ for 24 h. In some experiments, $2\times10^5$/ml sorted aorta monocytes were exposed to 50 μg/mL oxLDL for 24 h.

## Lentiviral transduction

Primary peritoneal macrophages were isolated from wild-type mice as described previously.[10,11] The ETV6 Mouse shRNA Plasmid (Cat# TL500638) and control plasmid containing the scramble shRNA sequence were purchased from OriGene. Lentiviral packaging and titration were conducted by Biofavor Biotech Co., Ltd. The lentivirus encoding ETV6 shRNA was termed LSh-E, whereas the lentivirus encoding the scramble shRNA was termed LSh-C. Before transduction, $4\times10^6$/ml peritoneal macrophages were seeded in a 6-well plate in the presence of 8 μg/mL polybrene (Sigma-Aldrich). LSh-E or LSh-C was added into macrophage cultures at the MOI of 10 and incubated for 16 h. Macrophages were then incubated in fresh RPMI1640 for 2 days. Puromycin (1 μg/mL, Sigma-Aldrich) was added to incubate macrophages for additional 2 days. After that, macrophages were cultured in fresh RPMI1640.

## oxLDL and cholesterol uptake assay

Peritoneal macrophages ($5\times10^5$/ml) were primed with 200 ng/mL LPS for 6h. The uptake of oxLDL and cholesterol was determined using the Oxidized LDL Uptake Assay Kit and Cholesterol Uptake Cell-Based Assay Kit, respectively, following the manufacturer's instructions. Briefly, macrophages were exposed to serum-free RPMI1640 containing oxLDL-DyLight™ 488 (1:50 dilution) or 20 μg/ml NBD cholesterol for 2 h at 37ºC. Macrophages were then washed with PBS, trypsinized with 0.25% Trypsin for 5 min, and fixed with 4% paraformaldehyde for 30 min in the darkness to remove the GFP signal. After that, oxLDL-DyLight™ 488 and NBD cholesterol were assessed using FACS.

## Immunoblotting

The whole-cell proteins were extracted by lysing cells in the RIPA buffer containing protease inhibitors and phosphatase inhibitors (Thermo Fisher) for 30 min on ice. Nuclear proteins were extracted using the Nuclear and Cytoplasmic Protein Extraction Kit (Beyotime Biotech). Briefly, cells were detached with 0.25% trypsin-EDTA and collected into a 1.5-ml Eppendorf tube. Cells were centrifuged at 250 r/min for 5 min and the cell pellet was incubated in 1× pre-extraction buffer (50 μl of buffer for $1\times10^6$ cells) on ice for 10 min. Cells were vortexed for 10 s and centrifuged at 12,000 r/min for 1 min. After discarding the supernatant, the nuclear pellet was incubated in 40 μl of 1× extraction buffer on ice for 15 min. The suspension was centrifuged at 14,000 r/min for 10 min at 4°C, and the supernatant was collected for Immunoblotting. The β-actin (sc-47,778) antibody was purchased from Santa Cruz Biotechnology. The ETV6 antibody (PA5-79,224) was purchased from Thermo Fisher Scientific. The phospho-IKKα/β (Ser176/180) antibody (2694), and IKKβ antibody (8943), IκBα antibody (4814), NF-κB p65 antibody (8242), phospho-NF-κB p65 (Ser536) (E1Z1T), and Lamin B2
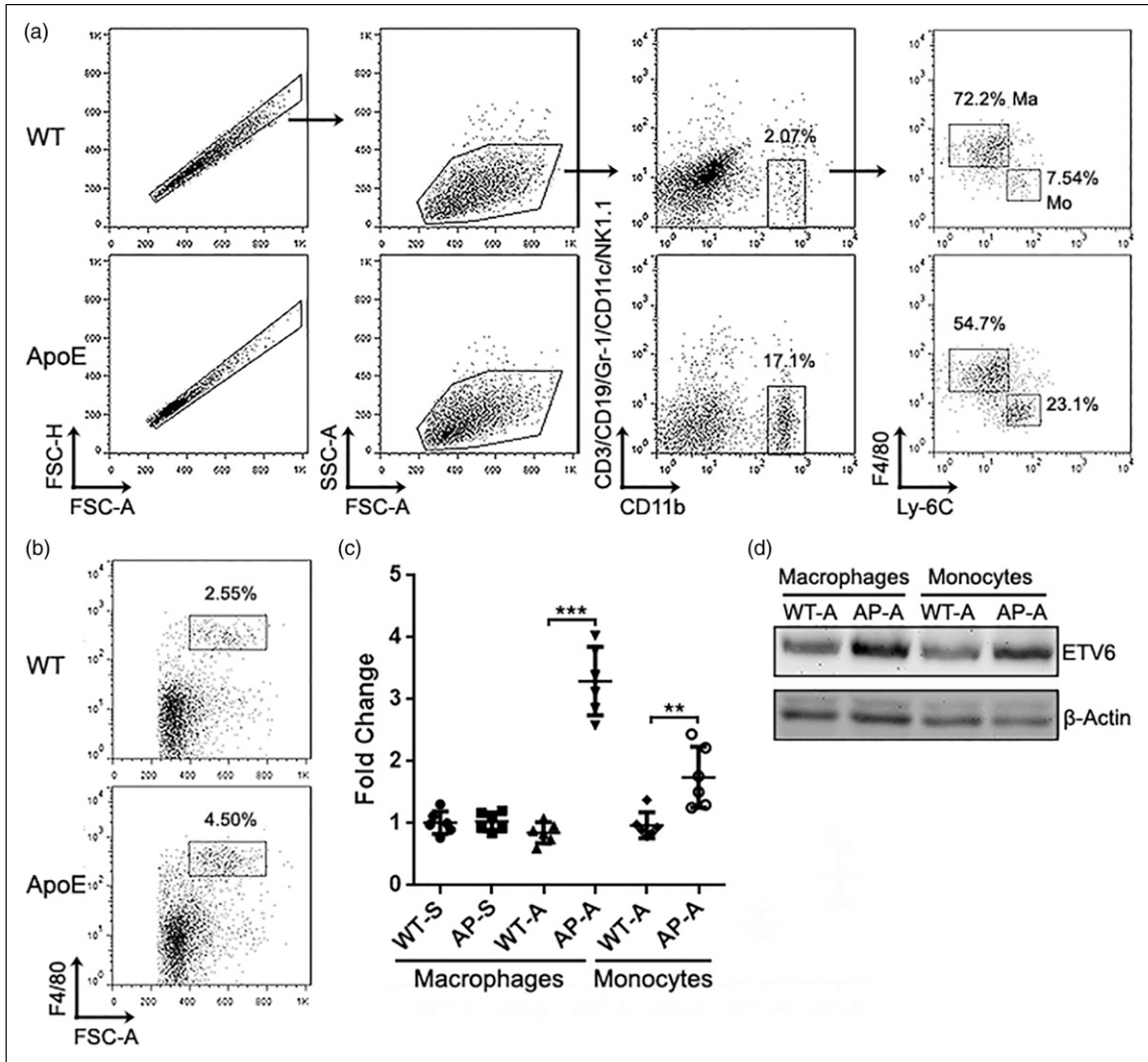
**Figure 1. ETV6 expression in aorta macrophages**. (a) FACS dot plots showing aorta macrophages and monocytes. Intact cells were gated within singlets, followed by gating CD3/CD19/Gr-1/CD11c/NK1.1$^-$CD11b$^+$ cells. Macrophages and monocytes were then recognized based on the expression of F4/80 and Ly-6C. WT: wild-type mice. ApoE: atherosclerotic ApoE$^{-/-}$ mice. Ma: macrophages. Mo: monocytes. (b) F4/80$^+$ macrophages in mouse spleens. (c) ETV6 mRNA in aorta macrophages and monocytes. WT-S: wild-type mouse spleen. AP-S: ApoE$^{-/-}$ mouse spleen. WT-A: wild-type mouse aorta. AP-A: ApoE$^{-/-}$ mouse aorta. N = 6 mice. *, $p$ <0.05; **, $p$ <0.01. (d) ETV6 protein in each cell population. The data represent two independent immunoblotting tests.

antibody (13,823) were purchased from Cell Signaling Technology. The results were recorded on an Azure c300 Gel Imaging System (Azure Biosystems) and quantified by the ImageJ.

### Caspase-1 activation assay

The active form of caspase-1 was quantified using the FLICA 660 Caspase-1 Kit (Bio-Rad). Macrophages were incubated in serum-free RPMI1640 containing FLICA 660 working solution (1:60 dilution) for 30 min at 37°C in the darkness. The FLICA 660 fluorescence intensity,

which signifies active caspase-1, was quantified by FACS.

### Adoptive transfer

ApoE$^{-/-}$ mice were given a high-fat diet for 16 weeks. Through retro-orbital injection, $5 \times 10^6$ lentivirus-infected macrophages resuspended in 150 μl of saline were injected into each mouse. The injection was repeated once 3 days later. Two weeks later, the recipients were euthanized and exogenous macrophages were retrieved from their spleens and aortas.

## Statistics

Every experiment was independently carried out two or 3 times. The data were shown as mean ± standard deviation. The Student's t-test or one-way ANOVA with post-hoc Tukey HSD test was used to compare the differences. A *p-value* <0.05 was considered significant. The minimum number of animals needed to attain statistical significance of *p* <0.05 with an 80% probability was calculated using the Sample Size & Power Calculator provided by the Chinese University of Hong Kong (http://www.lasec.cuhk.edu.hk/sample-size-calculation.html), based on the mean value and standard deviation of each group in the pilot study.

## Results

### Elevation of ETV6 in aorta macrophages in ApoE$^{-/-}$ mice

The oil red O staining showed a significant increase in atherosclerosis (oil red O-positive areas) in ApoE$^{-/-}$ mice fed with a high-fat diet, substantiating the establishment of the atherosclerosis model (Supplementary Figure 1). As shown in Figure 1(a), immune cells were isolated from the aortas of wild-type and atherosclerotic ApoE$^{-/-}$ mice. CD3/CD19/Gr-1/CD11c/NK1.1-positive cells, that is, T cells, B cells, neutrophils, dendritic cells, and NK cells were excluded by FACS. CD11b$^+$ cells in the CD3/CD19/Gr-1/CD11c/NK1.1-negative population were recognized as monocytes/macrophages. These cells were further divided into F4/80$^+$Ly-6C$^-$ macrophages and F4/80$^-$Ly-6C$^+$ monocytes. Splenic F4/80$^+$ macrophages were also sorted (Figure 1(b)). In atherosclerotic mice, the ETV6 mRNA was robustly up-regulated in aorta macrophages and moderately increased in aorta monocytes (Figure 1(c)). These increases were confirmed by Immunoblotting (Figure 1(d)). The abundant ETV6 expression in atherosclerotic macrophages was also demonstrated by immunofluorescent staining (Supplementary Figure 2).

### oxLDL and LPS promotes ETV6 expression in aorta macrophages

Aorta macrophages undergo functional changes after taking up oxLDL.[12-14] Therefore, we tested if oxLDL changes ETV6 expression in macrophages by treating wild-type aorta macrophages with oxLDL. As shown in Figure 2(a), oxLDL increased ETV6 mRNA by over three folds. Interestingly, LPS up-regulated ETV6 mRNA by nearly two folds. However, we did not observe any synergistic effect of oxLDL plus LPS. The ETV6-inducing effect of oxLDL and LPS were proved by Immunoblotting (Figure 2(b)). Because the NF-κB pathway is activated by oxLDL and LPS, we thought it might be related to the change in ETV6. To test this hypothesis, macrophages were treated with oxLDL or LPS in the presence or absence of the NF-κB inhibitor QNZ. As shown in Figure 2(c) and (d), QNZ significantly suppressed oxLDL- or LPS-mediated ETV6 up-regulation, suggesting that the NF-κB pathway is indeed involved in ETV6 up-regulation. Similarly, oxLDL also significantly boosted ETV6 mRNA in sorted aorta monocytes while enhancing the mRNA levels of pro-inflammatory cytokines such as IL-1β, IL-6, and TNF-α (Supplementary Figure 3).

### Lentivirus-mediated ETV6 knockdown in macrophages

To elucidate the role of ETV6, we transduced wild-type peritoneal macrophages with lentiviral particles that encode both ETV6 shRNA and GFP. The transduction efficiency was over 50% before puromycin selection, according to the proportion of GFP-expressing cells (Figure 3(a)). After puromycin selection, over 90% of macrophages were GFP-positive (Figure 3(a) and (b)). The transduced macrophages were then incubated in a fresh medium for additional 2 days until virus-induced inflammatory response disappeared. At this time point, the expression of both pro-inflammatory cytokines such as IL-1β, IL-6, and TNF-α, as well as anti-inflammatory cytokines such as IL-10 and TGF-β were comparable in control lentivirus (LSh-C)-transduced macrophages and LSh-E-transduced macrophages (Figures 3(c) to (g)). Macrophage apoptosis and necrosis were not remarkably impacted by ETV6 knockdown (Figure 3(h)).

### ETV6 knockdown suppresses oxLDL-induced inflammatory reaction in vitro

As shown in Figure 4(a) and (b), ETV6 expression was remarkably reduced after transduction with ETV6 shRNA-encoding lentivirus (Lsh-E). oxLDL increased ETV6 expression in LSh-C-transduced macrophages but not in ETV6 LSh-E-transduced macrophages (Figure 4(a) and (b)), suggesting that ETV6 knockdown was stable under oxLDL exposure. In agreement with the previous study,[15] oxLDL significantly boosted the expression of IL-1β, IL-6, and TNF-α in LSh-C-transduced macrophages. However, this pro-inflammatory effect was markedly weaker in LSh-E-macrophages (Figures 4(c) to (e)), indicating that ETV6 played a significant role in an oxLDL-induced inflammatory reaction in macrophages. The uptake of either oxLDL or cholesterol was not significantly affected after the ETV6 knockdown (Figure 4(f) and (g)).
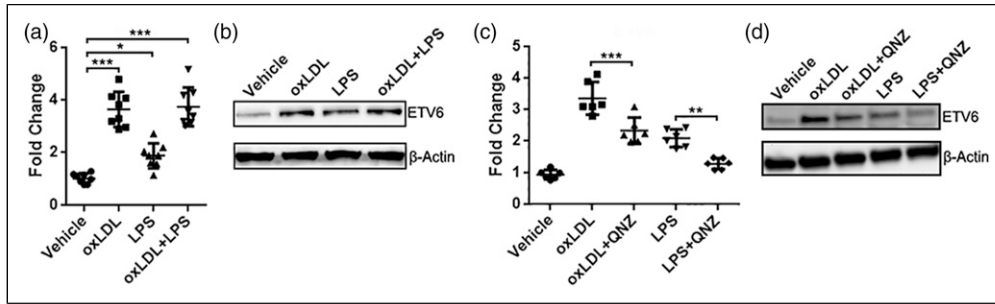
**Figure 2. ETV6 expression in aorta macrophages after oxLDL and/or LPS treatment. (a)** ETV6 mRNA in wild-type aorta macrophages after incubation with oxLDL and/or LPS. N=8 mice. **(b)** ETV6 protein in aorta macrophages. **(c)** ETV6 mRNA in aorta macrophages after treatment in the presence or absence of QNZ. **(d)** ETV6 protein in aorta macrophages after treatment in the presence or absence of QNZ. N = 6 samples. *, $p<0.05$; **, $p<0.01$; ***, $p<0.001$.
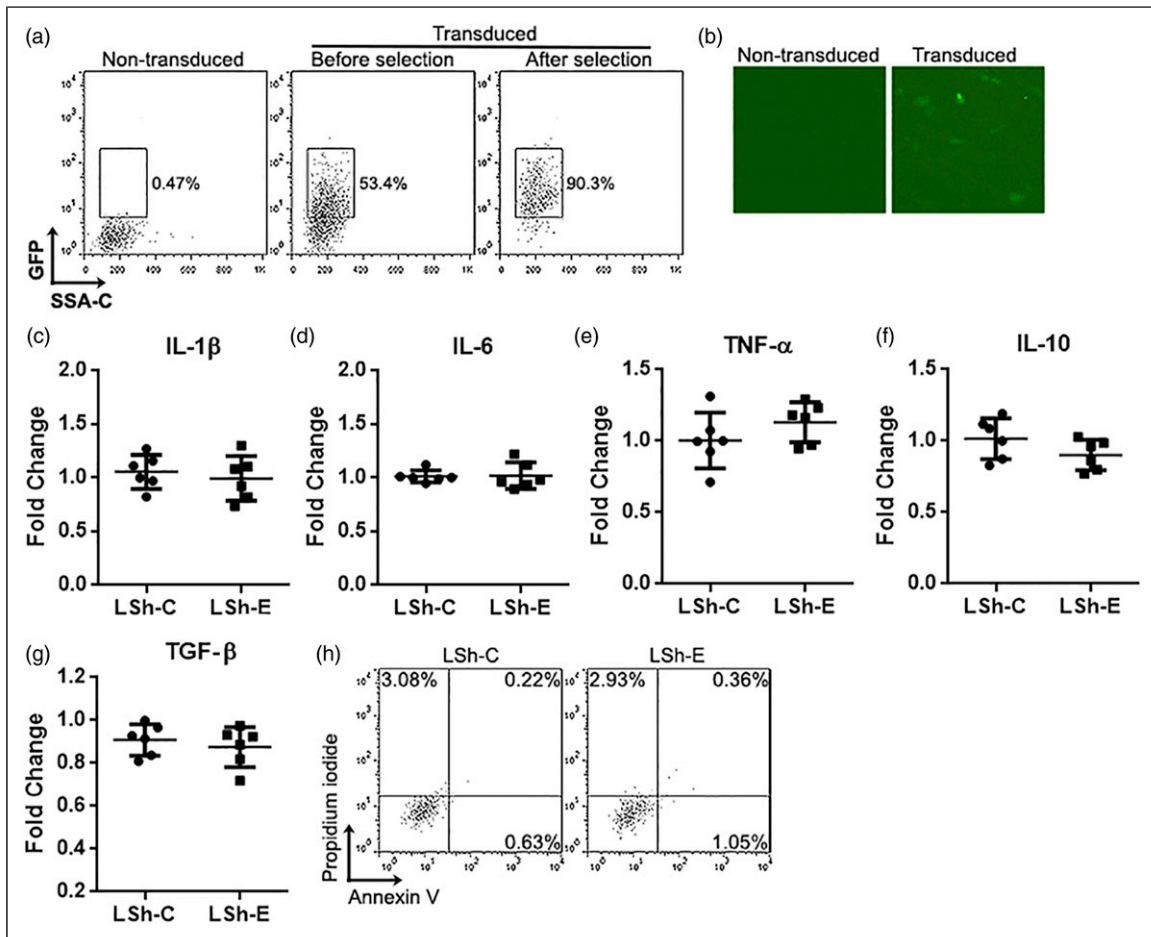


**Figure 3. Lentivirus-mediated ETV6 knockdown. (a)** FACS dot plots indicating GFP expression in non-transduced peritoneal macrophages and LSh-E-transduced peritoneal macrophages 2 days after transduction (before puromycin selection) and 4 days after transduction (2 days after puromycin selection). **(b)** Fluorescent microscopy showing GFP expression in macrophages. Original magnification = 100×. **(c to g)** The expression of indicated cytokines in macrophages 6 days after transduction. N = 6. **(h)** Cell death in macrophages. The data represent two independent FACS experiments.
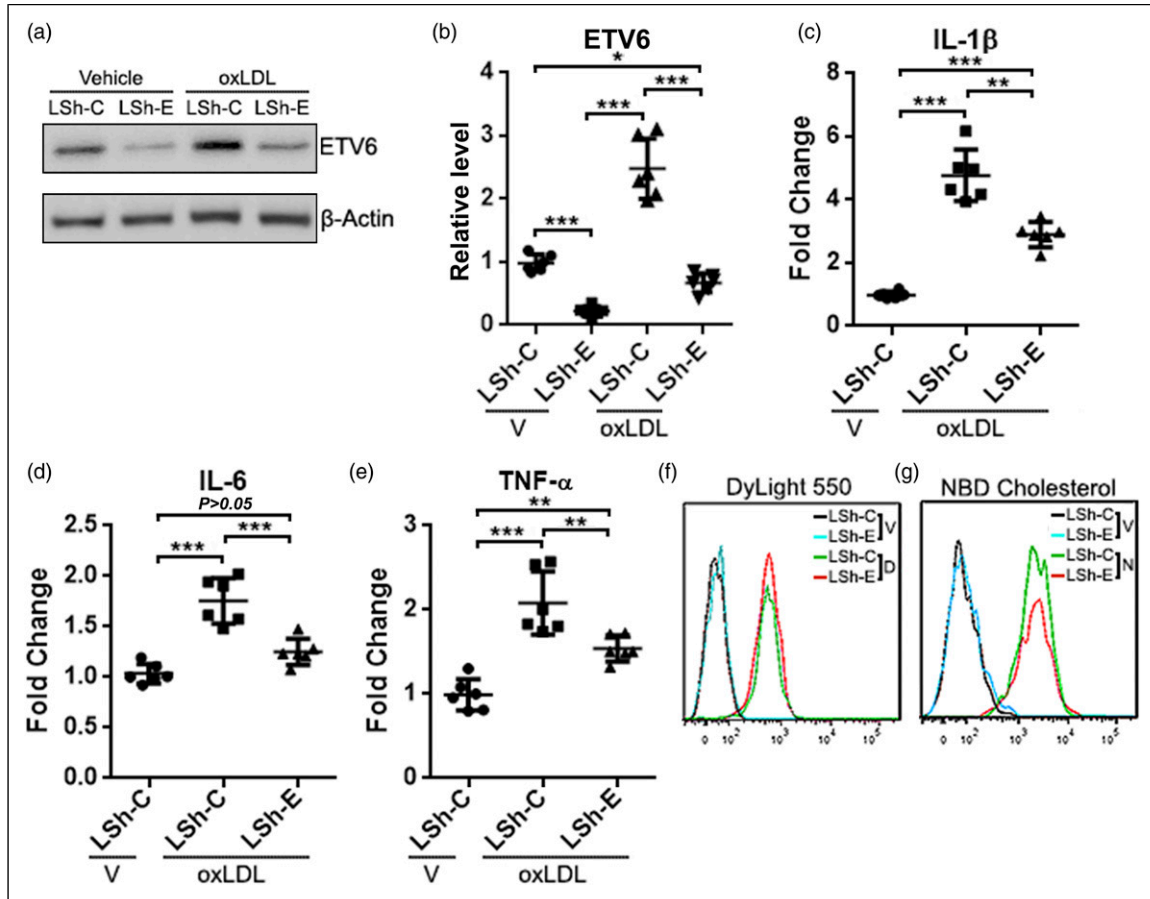
**Figure 4.** Effect of ETV6 knockdown on oxLDL-induced inflammatory reaction in macrophages *in vitro*. **(A and B)** ETV6 protein in macrophages after vehicle or oxLDL treatment. Representative Immunoblotting images are shown in (a). Statistics are shown in (b). LSh-C: LSh-C-transduced macrophages. LSh-E: LSh-E-transduced macrophages. **(c to e)** The expression of indicated cytokines in macrophages. N = 6. *, $p < 0.05$; **, $p < 0.01$; ***, $p < 0.001$. **(F and G)** FACS histograms indicating the uptake of oxLDL (f) and cholesterol (g) by macrophages. V: vehicle. D: DyLight 550 oxLDL. N: NBD cholesterol. The data represent two independent FACS experiments.

## ETV6 knockdown impairs oxLDL-induced activation of the NF-κB pathway

The NF-κB pathway is essential to oxLDL-induced response in macrophages.[15] To check whether it is crucial to the effect of ETV6, we first analyzed the phosphorylation of IKKβ. As shown in Figure 5(a) and (b), in vehicle-treated groups, the baseline IKKβ phosphorylation was comparable in LSh-C-transduced macrophages and LSh-E-transduced macrophages. oxLDL promoted IKKβ phosphorylation in both LSh-C-transduced macrophages and LSh-E-transduced macrophages. However, LSh-E-transduced macrophages had less phosphorylated IKKβ than LSh-C-transduced macrophages after oxLDL treatment. Consistently, oxLDL also increased the phosphorylation of NF-κB p65 in LSh-C-transduced macrophages. However, oxLDL-induced p65 phosphorylation was suppressed in

LSh-E-transduced macrophages (Figure 5(a) and (c)). We then measured the amount of IκBα and found that oxLDL decreased IκBα in both LSh-C-transduced macrophages and LSh-E-transduced macrophages, whereas LSh-E-transduced macrophages had more IκBα than LSh-C-transduced macrophages (Figure 5(d) and (e)). After oxLDL exposure, the amount of nuclear NF-κB p65 was significantly increased in LSh-C-transduced macrophages and less significantly increased in LSh-E-transduced macrophages (Figure 5(d) and (f)). The change in nuclear p65 was also observed by Immuno-fluorescence cytochemistry (Supplementary Figure 4). Because the NF-κB pathway participates in the activation of inflammasomes and Caspase-1,[16] we determined the levels of active Caspase-1 using FACS. As shown in Figure 5(g) an average of 13.76% of LSh-C-transduced macrophages expressed active Caspase-1 after oxLDL treatment, while only 10.34% of LSh-E-transduced
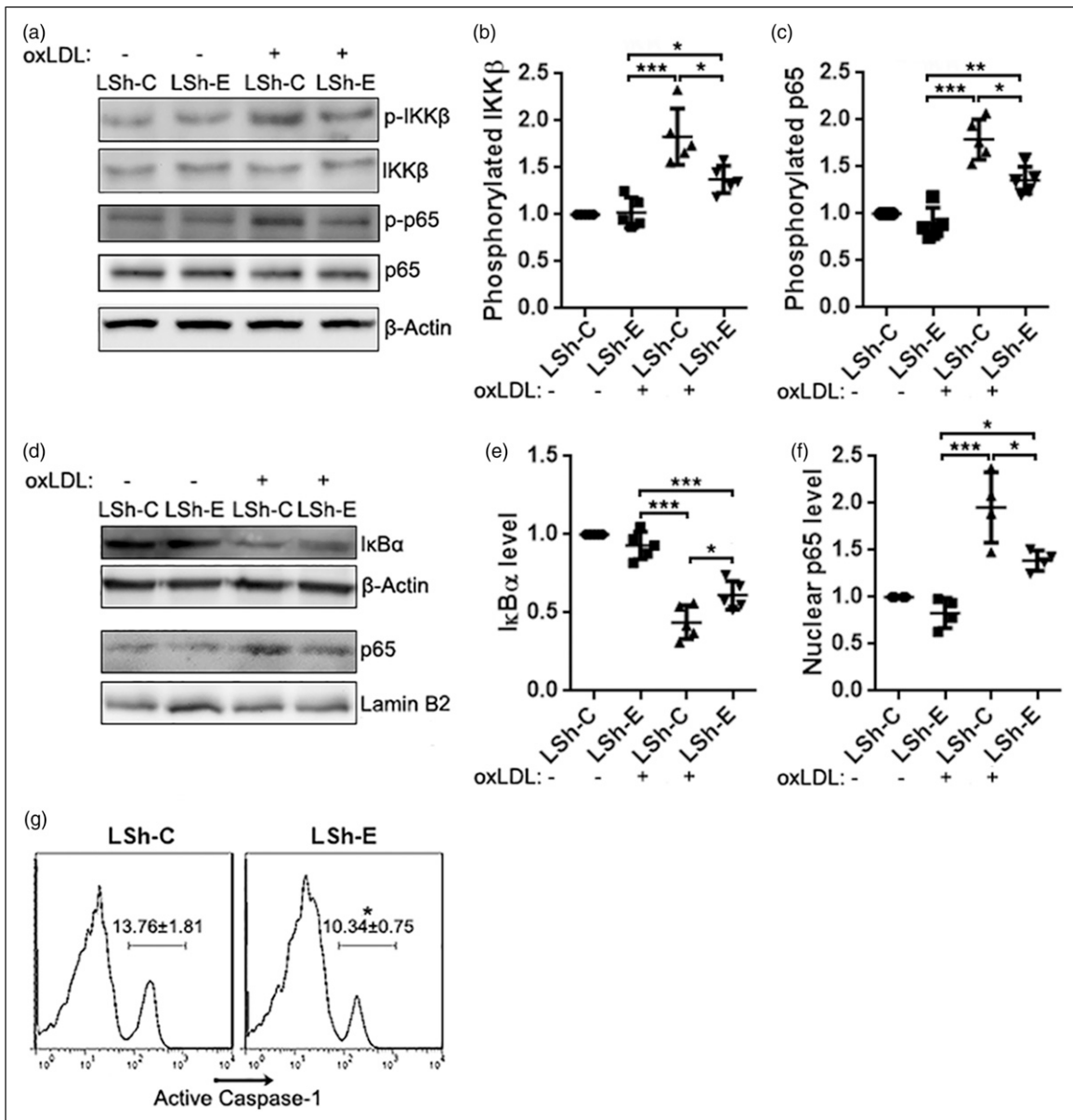
**Figure 5. Impact of ETV6 knockdown on oxLDL-induced NF-κB pathway. (A to C)** Phosphorylation of IKKβ (Ser180) and NF-κB p65 (Ser536) in macrophages after oxLDL treatment. Immunoblotting images are shown in (a), and statistics are shown in (b) and (c), respectively. LSh-C: LSh-C-transduced macrophages. LSh-E: LSh-E-transduced macrophages. **(D to F)** Expression of IκBα and nuclear NF-κB p65 in macrophages. Immunoblotting images are shown in (d), and statistics of IκBα and nuclear NF-κB p65 levels are shown in (e and f), respectively. N = 5. **(g)** FACS histograms indicating the expression of active Caspase-1 in macrophages after oxLDL treatment. N = 6. *, $p < 0.05$; ***, $p < 0.001$.

macrophages expressed active Caspase-1. Therefore, activation of the NF-κB pathway and inflammasomes were suppressed in LSh-E-transduced macrophages. Moreover, when stimulated with M-CSF, LSh-E-transduced macrophages exhibited fewer Ki67$^+$ cells than LSh-C-transduced macrophages, suggesting that ETV6 knockdown suppressed macrophage proliferation (Supplementary Figure 5).

## ETV6 knockdown suppresses aorta macrophage-mediated inflammatory reaction in vivo

To test the role of ETV6 *in vivo*, we infused lentivirus-transduced macrophages into ApoE$^{-/-}$ mice after atherosclerosis was formed. Two weeks after infusion, the atherosclerotic recipients were euthanized and GFP-expressing exogenous
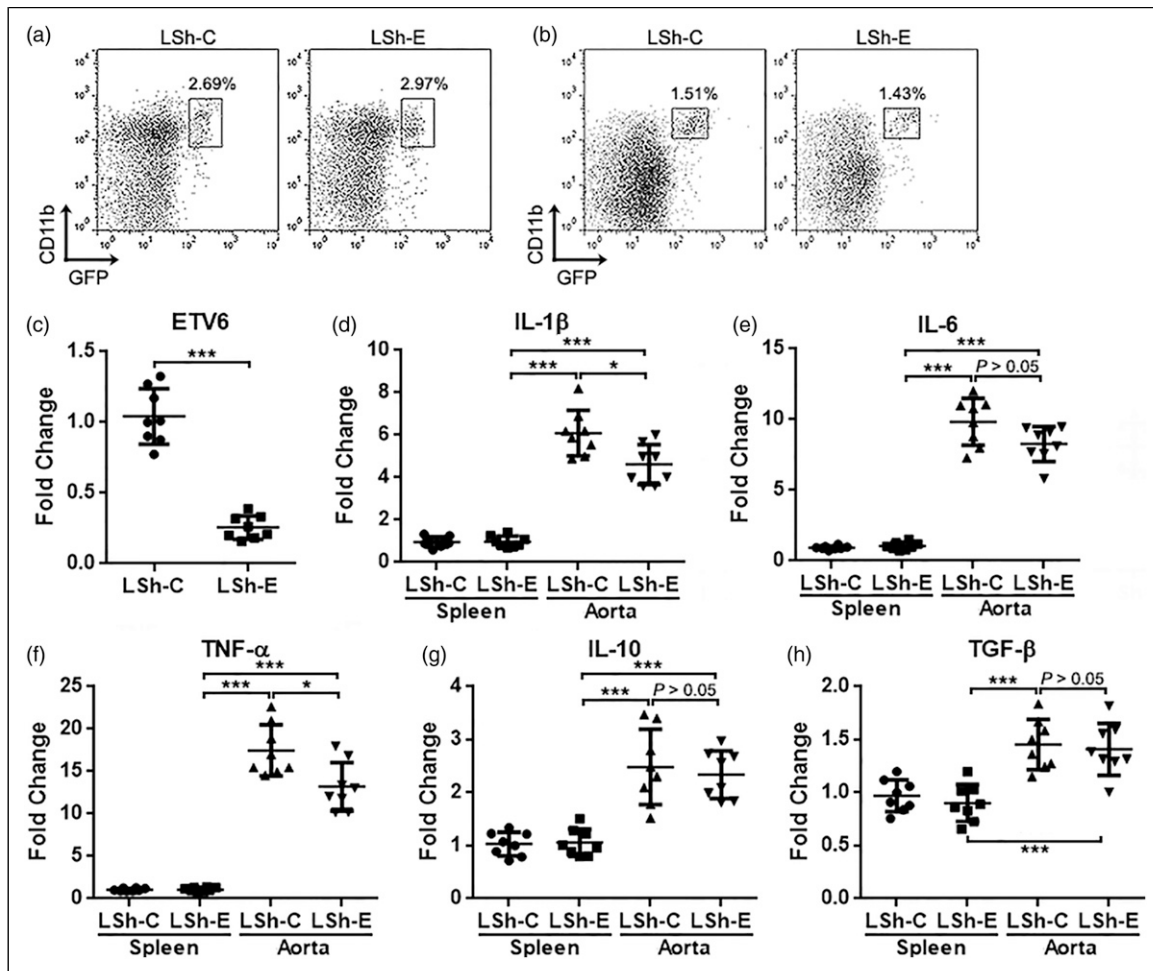
**Figure 6. Effect of ETV6 knockdown *in vivo*. (A and B)** FACS dot plots indicating recognizing and sorting exogenous GFP⁺ macrophages from aorta mononuclear cells (a) and splenocytes (b) of recipient mice. LSh-C: mice receiving LSh-C-transduced macrophages. LSh-E: mice receiving LSh-E-transduced macrophages. **(c)** ETV6 mRNA in sorted exogenous GFP⁺ macrophages. **(d to h)** The expression of indicated cytokines in sorted exogenous GFP⁺ macrophages. N = 8 mice. *, $p < 0.05$; ***, $p < 0.001$.

macrophages were retrieved from the aortas and spleens by FACS. We observed comparable percentages of LSh-C-transduced macrophages and LSh-E-transduced macrophages in the recipients (Figure 6(a) and (b)), suggesting that ETV was not involved in macrophage migration. ETV6 knockdown persisted in LSh-E-transduced macrophages (Figure 6(c)). The mRNA abundances of IL-1β, IL-6, TNF-α, IL-10, and TGF-β in exogenous macrophages were then evaluated by RT-qPCR. As shown in Figures 6(d) to (f), IL-1β, IL-6, and TNF-α were up-regulated in aorta LSh-C-transduced macrophages relative to their splenic counterparts. However, in aorta LSh-E-transduced macrophages, the expression of IL-1β and TNF-α were not as high as those in LSh-C-transduced macrophages. Production of IL-10 and TGF-β were moderately increased in exogenous aorta macrophages and seemed comparable in LSh-C-transduced

macrophages and LSh-E-transduced macrophages (Figure 6(g) and (h)).

## Discussion

The behavior of macrophages in the progression and regression of atherosclerotic lesions is a persistent hotspot in atherosclerosis research. Advanced technologies and methods have been applied to modulate the inflammatory reaction of macrophages to control the formation of atherosclerotic plaques, including the single-chain variable fragment antibody targeting oxidation-specific epitopes.[17] As a transcription factor, ETV6 contains two functional domains: an N-terminal pointed domain involved in protein-protein interactions with itself and other proteins, and a C-terminal DNA-binding domain. Although Gene knockout studies demonstrate its crucial role

in hematopoiesis and vasculature development,[18,19] the effect of ETV6 in the regulation of adult immune cells remains unknown.

Our first discovery is the elevation of ETV6 expression in atherosclerotic macrophages in the aorta. To our understanding, we are the first to report this change in the field. It should be noted that besides macrophages, infiltrating monocytes also up-regulated ETV6 expression in comparison to their counterparts in the bloodstream. The microenvironment of the atherosclerotic aorta could up-regulate ETV6. Furthermore, we identified that oxLDL and LPS were able to induce ETV6 in aorta macrophages via activating the NF-κB pathway. The NF-κB pathway is essential for inflammatory responses because it mediates the induction of various pro-inflammatory genes in innate immune cells.[20] Therefore, perhaps the change in ETV6 reflects the pro-inflammatory status of aorta macrophages and infiltrating monocytes. In the future, it is necessary to determine whether NF-κB p65 and p50 directly initiate ETV6 expression by binding to the promoter/enhancer region of the *ETV6* gene, or indirectly by regulating other factors that promote ETV6 transcription. It will also be interesting to evaluate ETV6 expression in other macrophage-mediated inflammatory disorders such as inflammatory bowel disease and arthritis.

Another appealing finding is the significantly positive effect of ETV6 on oxLDL-triggered inflammatory response in macrophages. Upon uptake of oxLDL, an array of inflammatory biomarkers and mediators are escalated in macrophages.[13,21] Our ETV6 knockdown experiments indicated that ETV6 knockdown seemed not to influence the inflammatory reaction in resting macrophages. However, ETV6 enhanced the production of pro-inflammatory cytokines after oxLDL exposure. We thus concluded that oxLDL and ETV6 form a positive cascade of inflammatory reaction: engulfed oxLDL promotes ETV6 expression and ETV6 further augments oxLDL-induced inflammation. Nonetheless, the ETV6 knockdown did not alter the uptake of either oxLDL or cholesterol, suggesting that ETV6 did not affect the expression of oxLDL receptors and the pinocytosis mechanism.

Furthermore, we identified that the NF-κB pathway is downstream of ETV6. Because ETV6 is a transcription factor, it could not impact the NF-κB signaling directly. ETV6 likely modulates the expression of the molecule(s) that correlates to the NF-κB pathway. Unfortunately, the targets of ETV6 remain unknown. Recent research reports that myeloid differentiation factor 2 (MD2) is required for oxLDL-induced TLR4 activation and inflammation via directly binding to ox-LDL.[22] MD2, also known as lymphocyte antigen 96 (LY96), is a protein associated with toll-like receptor four on the cell surface. Interestingly, we analyzed the transcription factor binding sites on the promoter/enhancer region of the *LY96* gene and found a putative

ETV6 binding site (data not shown). Hence, it is probable that ETV6 drives the expression of MD2 to promote oxLDL-TLR4 ligation and downstream NF-κB signaling. The NF-κB pathway then stimulates the formation of inflammasomes and subsequent activation of Caspase-1, causing the expression of a series of inflammatory cytokines. Our ongoing study is testing this hypothesis.

However, this study has some limitations. First, the temporal change in ETV6 expression is still unknown because this study only addressed ETV6 expression in aorta macrophages before and after atherosclerosis. So whether ETV6 expression is dynamically associated with aorta macrophage activity is not elucidated. Second, the effect of ETV6 on the development of atherosclerotic lesions is not revealed. If possible, a macrophage-specific ETV6-knockout mouse strain could be used to investigate atherosclerosis in the future. Third, the study did not check ETV6 expression in different macrophage subsets. Therefore, it is unclear whether ETV6 differentially impacts the functions of M1, M2, M4, and other macrophage subsets. Further investigations should answer these questions.

In conclusion, the present study suggests that in atherosclerotic lesions, oxLDL induces the up-regulation of ETV6 in macrophages via the NF-κB pathway. Subsequently, ETV6 promotes the NF-κB signaling to amplify the inflammatory response, thus forming positive feedback of the NF-κB signaling. Our endeavor has revealed a novel mechanism by which the pro-inflammatory activity of atherosclerotic macrophages is enhanced.

## Conclusion

In a murine atherosclerosis model, we characterized the expression and function of ETV6 in aorta macrophages. We found that ETV6 was up-regulated in aorta macrophages in atherosclerotic lesions. Additional experiments indicated that uptake of oxLDL increased ETV6 expression in macrophages and ETV6 supports oxLDL-induced inflammatory response in macrophages probably through promoting oxLDL-induced activation of NF-κB signaling. Although there were some limitations in our study, such as the lack of information on the temporal change of ETV6 in macrophage subsets, the current study suggested that ETV6 positively regulates macrophage-mediated inflammation in atherosclerotic lesions. Therefore, we revealed a novel mechanism by which the pro-inflammatory activity of atherosclerotic macrophages is maintained and enhanced.

## Authors' contributions

analyzed by Xiaofang Xiong. Several in vitro experiments were carried out by Zheng Yan. RNA extraction, cDNA preparation, and RT-qPCR were performed by Wei Jiang.

## ORCID iD

Xiaofang Xiong https://orcid.org/0000-0001-9039-5576

## Supplemental Material

Supplemental material for this article is available online.

## References

1. Sukhorukov VAK VN, Chegodaev YS, Ivanova E, et al. (2020) Lipid metabolism in macrophages: focus on atherosclerosis. *Biomedicines* 8: 262. DOI: 10.3390/biomedicines8080262.
2. IaIi A (2019) Immunity and inflammation in atherosclerosis. *Circulation Research* 124: 315–327. DOI: 10.1161/CIRCRESAHA.118.313591.
3. KathrynMoore JIT (2011) Macrophages in the pathogenesis of atherosclerosis. *Cell* 145: 341–355. DOI: 10.1016/j.cell.2011.04.005.
4. KathrynMoore JFJS and Fisher EA (2013) Macrophages in atherosclerosis: a dynamic balance. *Nature Reviews Immunology* 13: 709–721. DOI: 10.1038/nri3520.
5. Lei Bi TM, Xu L, Lai W, et al. (2021) New progress in the study of germline susceptibility genes of myeloid neoplasms. *Oncology letters* 21: 317. DOI: 10.3892/ol.2021.12578.
6. Federica Melazzini FP, Balduini A, De Rocco D, et al. (2016) Anna Savoia clinical and pathogenic features of ETV6-related thrombocytopenia with predisposition to acute lymphoblastic leukemia. *Haematologica* 101: 1333–1342. DOI: 10.3324/haematol.2016.147496.
7. Takaya Moriyama MLM, Wu G, Nishii R, et al. (2015) Germline genetic variation in ETV6 and risk of childhood acute lymphoblastic leukaemia: a systematic genetic study. *Lancet Oncology* 16: 1659–1666. DOI: 10.1016/S1470-2045(15)00369-1.
8. MatthewButcher JMH, Ley K and Galkina E (2011) Flow cytometry analysis of immune cells within murine aortas. *Journal of Visualized Experiments* 53: 2848. DOI: 10.3791/2848.
9. Breanne N Gjurich PLT-M and V Galkina E (2015) Flow cytometric analysis of immune cells within murine aorta. *Methods in Molecular Biology* 1339: 161–175. DOI: 10.1007/978-1-4939-2929-0_11.
10. Pan Y, Wang Y, Cai L, et al. (2012) Inhibition of high glucose-induced inflammatory response and macrophage infiltration by a novel curcumin derivative prevents renal injury in diabetic rats. *Br J Pharmacol* 166: 1169–1182. DOI: 10.1111/j.1476-5381.2012.01854.x.
11. Zhang X, Goncalves R and Mosser DM (2008) The isolation and characterization of murine macrophages. *Curr Protoc Immunol*: 11. Chapter 14: Unit 14. DOI: 10.1002/0471142735.im1401s83.
12. van Tits RS LJH, van Lent PL, Netea MG, et al. (2011) Oxidized LDL enhances pro-inflammatory responses of alternatively activated M2 macrophages: a crucial role for Krüppel-like factor 2. *Atherosclerosis* 214: 345–349. DOI: 10.1016/j.atherosclerosis.2010.11.018.
13. Oscar J, Lara-Guzmán ÁG- I, Medina S, et al. (2018) Oxidized LDL triggers changes in oxidative stress and inflammatory biomarkers in human macrophages. *Redox Biology* 15: 1–11. DOI: 10.1016/j.redox.2017.11.017.
14. Anja Schwarz GAB and Schwarzbach H (2017) Ralf Kinscherf oxidized LDL-induced JAB1 influences NF-κB independent inflammatory signaling in human macrophages during foam cell formation. *Journal of Biomedical Science* 24: 12. DOI: 10.1186/s12929-017-0320-5.
15. Chen T, Huang W, Qian J, et al. (2020) Macrophage-derived myeloid differentiation protein 2 plays an essential role in ox-LDL-induced inflammation and atherosclerosis. *EBioMedicine* 53: 102706. DOI: 10.1016/j.ebiom.2020.102706.
16. Ting Liu LZ, Joo D and Sun S-C (2017) NF-κB signaling in inflammation. *Signal transduction and targeted therapy* 2: 17023. DOI: 10.1038/sigtrans.2017.23.
17. Zhang L, Xue S, Ren F, et al. (2021) An atherosclerotic plaque-targeted single-chain antibody for MR/NIR-II imaging of atherosclerosis and anti-atherosclerosis therapy. *J Nanobiotechnology* 19: 296. DOI: 10.1186/s12951-021-01047-4.
18. Hanno Hock EM, Medeiros S, Schindler JW, et al. (2004) Tel/Etv6 is an essential and selective regulator of adult

hematopoietic stem cell survival. *Genes & Development* 18: 2336–2341. DOI: 10.1101/gad.1239604.

19. Lei Li RR (2019) Roger patient, Aldo Ciau-Uitz, Catherine Porcher Etv6 activates vegfa expression through positive and negative transcriptional regulatory networks in xenopus embryos. *Nature communications* 10: 1083. DOI: 10.1038/s41467-019-09050-y.

20. Koji Taniguchi MK (2018) NF-κB, inflammation, immunity and cancer: coming of age. *Nature Reviews Immunology* 18: 309–324. DOI: 10.1038/nri.2017.142.

21. JillianRhoads ASM P (2018) How Oxidized Low-Density Lipoprotein Activates Inflammatory Responses. *Critical Reviews in Immunology* 38: 333–342. DOI: 10.1615/CritRevImmunol.2018026483.

22. Taiwei Chen WH, Qian J, Luo W, et al. Guang Liang macrophage-derived myeloid differentiation protein 2 plays an essential role in ox-LDL-induced inflammation and atherosclerosis. *EBioMedicine* 2020; 53: 102706. DOI: doi: 10.1016/j.ebiom.2020.102706.